Brown Seaweed Sargassum-Based Sorbents for the Removal of Cr(III) Ions from Aqueous Solutions

Natalia Niedzbala, Katarzyna Dziergowska, Maja Welna, Anna Szymczycha-Madeja, Jacek Chęcmanowski, Nathalie Bourgougnon, Izabela Michalak

processes

MDPI

Article

Brown Seaweed *Sargassum*-Based Sorbents for the Removal of Cr(III) Ions from Aqueous Solutions

Natalia Niedzbała [1], Katarzyna Dziergowska [1], Maja Wełna [2,*], Anna Szymczycha-Madeja [2], Jacek Chęcmanowski [1], Nathalie Bourgougnon [3] and Izabela Michalak [1]

[1] Department of Advanced Material Technologies, Faculty of Chemistry, Wroclaw University of Science and Technology, Smoluchowskiego 25, 50-372 Wroclaw, Poland
[2] Department of Analytical Chemistry and Chemical Metallurgy, Faculty of Chemistry, Wroclaw University of Science and Technology, Wybrzeze St. Wyspianskiego 27, 50-370 Wroclaw, Poland
[3] Laboratoire de Biotechnologie et Chimie Marines, Université Bretagne Sud, EMR 6076, IUEM, 56000 Vannes, France
* Correspondence: maja.welna@pwr.edu.pl

Abstract: In this study, zinc oxide nanoparticles (ZnO NPs) were biosynthesized with the use of an extract derived from seaweed (*Sargassum* sp.) and used as a sorbent for the removal of Cr(III) ions from wastewater. The biosorption properties of the seaweed itself as well as of the post-extraction residue were investigated for comparison. ZnO NPs were characterized with UV–vis, ICP-OES, FTIR, XRD, and SEM techniques. The sorption capacity of the (bio)sorbents was investigated as a function of contact time at different pH values and initial concentrations of metal ions. Sorption kinetics and isotherms were studied in order to comprehend the sorption nature and mechanism. The sorption kinetic data were well-fitted with the pseudo-second-order model, and the highest sorption capacity was calculated for ZnO NPs (137 mg/g), whereas those calculated for *Sargassum* sp. (82.0 mg/g) and the post-extraction residue (81.3 mg/g) were comparable (at pH 5 and 300 mg of Cr(III) ions/L). The adsorption isotherms for all sorbents were well described using the Langmuir model. According to these findings, ZnO NPs were superior to the sorption properties of the tested biosorbents and can be used as a potential sorbent for the removal of metal ions from wastewater. Renewable seaweed biomass can be used for the sustainable biosynthesis of nanoparticles used for environmental protection.

Keywords: seaweed; extraction; nanoparticles biosynthesis; Cr(III) ions sorption; wastewater

Citation: Niedzbała, N.; Dziergowska, K.; Wełna, M.; Szymczycha-Madeja, A.; Chęcmanowski, J.; Bourgougnon, N.; Michalak, I. Brown Seaweed *Sargassum*-Based Sorbents for the Removal of Cr(III) Ions from Aqueous Solutions. *Processes* **2023**, *11*, 393. https://doi.org/10.3390/pr11020393

Academic Editor: Clara Grosso

Received: 16 December 2022
Revised: 18 January 2023
Accepted: 20 January 2023
Published: 27 January 2023

1. Introduction

Industrial and domestic waste effluents contain inorganic pollutants. Heavy metal ions in industrial wastewater are particularly dangerous and may pose a threat to humans and the natural environment. One of these elements is chromium, which is widely utilized in metallurgy, electroplating, the manufacture of paints and pigments, leather tanning, the preservation of wood, and the manufacture of chemicals, pulp, and paper [1–4]. There are several methods that are used for the removal of heavy metal ions from wastewater, including chemical precipitation, coagulation, flocculation, adsorption, electrodialysis, membrane separation, etc. [2–7]. Each method has a number of restrictions in terms of cost, complexity, and efficiency [3,7]. Adsorption is reported to have low operating costs, a high removal capacity, easy implementation, and to enable sorbent regeneration. Sorption is a process that relies on the ability to absorb and retain one substance by another. The sorption capacity is designated as the quantity of sorbate (metal ions) per unit mass of sorbent (e.g., [4,6,8–11]). In this process, both synthetic and natural adsorbents can be used, although the latter are very popular due to their low cost and widespread occurrence. Such an example would be the biomass of brown seaweed *Sargassum* sp., which has already

been used for the removal of Pb(II) [8], Fe(III) [9], Ni(II) [10], Cu(II) [10], Cr(III) [11–13], and Cr(VI) ions [14].

In recent years, there has been a growing interest to apply metal oxide nanoparticles (NPs) as sorbents of metal ions due to their small size and large surface area offering numerous active sites for the binding of metal ions [2,4,6,7]. There are several methods for metallic nanoparticle production: chemical methods known as the "bottom-up approach", whereby NPs are synthesized through chemical reactions between atoms, ions, and molecules; physical methods known as the "top-down approach", which involve the mechanical crushing/breaking down of the bulk material into NPs; and, finally, biological methods, which utilize microorganisms, enzymes, plants, and algae, and their extracts responsible for the reduction of metal precursors [6,15–18]. Metallic nanoparticles biosynthesized with the use of seaweed extracts could be an alternative to chemical and physical methods in terms of environmental and economic benefits; these extracts are safe, nonhazardous, environmentally friendly, and cost-effective. Additionally, biologically active compounds such as polyphenols, polysaccharides, fiber, protein, lipids, and vitamins in *Sargassum* sp. biomass offer several functional groups such as carboxyl and hydroxyl sulfate and amino, which play important roles in the formation and stabilization of nanoparticles [6,15,18].

Lately, zinc oxide nanoparticles (ZnO NPs) have received a lot of attention because of their unique properties and applications. Metal nanoparticles are more often analyzed for their use in the pharmaceutical and biomedical fields and in the cosmetic industry (cosmetics and sunscreen) [15,17,18]. Zinc nanoparticles are also known to possess antimicrobial (Gram-positive: *Staphylococcus aureus*, and *Bacillus cereus*; Gram-negative: *Escherichia coli*, and *Salmonella typhi*), antifungal properties (e.g., *Candida albicans* and *Aspergillus niger*), and antioxidant activity [18]. However, the sorption properties of nanoparticles have not yet been thoroughly investigated. So far, ZnO NPs synthesized chemically have been used for the sorption of Cu(II) [7] and Cr(VI) [5], as well as Zn(II), Cd(II), and Hg(II) [2], ions; hydrothermally for the sorption of Ni(II), Pb(II), Cu(II), and Cr(III) ions [4]; biologically, from green macroalga (*Cladophora glomerata*) for the sorption of Cr(III) ions [19] or from zerumbone (a phytochemical isolated from the *Zingiberaceae* family) for the sorption of Pb(II) ions [6]. To the best of our best knowledge, there is no information on the sorption properties of ZnO NPs biosynthesized from brown seaweeds.

The aim of the present study was to biosynthesize ZnO NPs using the *Sargassum* sp. extract and to examine them as a low-cost adsorbent for the removal of Cr(III) ions from aqueous solutions. Additionally, the sorption properties of the raw dry *Sargassum* sp. biomass, as well as the post-extraction residue obtained during the *Sargassum* sp. ultrasound-assisted extraction, were compared. The residue originating from seaweed extraction is usually discarded or used for the production of animal feed but is also randomly exploited as a biosorbent of heavy metal ions [3,19–21]. ZnO NPs were characterized using several techniques such as ICP-OES, FTIR, XRD, and SEM and were examined in terms of their sorption properties. The effects of pH and the initial concentration of metal ions in the solution on the sorption capacities of ZnO NPs, *Sargassum* sp., and the *Sargassum* sp. post-extraction residue were extensively investigated and compared.

2. Materials and Methods

2.1. Chemicals

Zinc(II) sulfate(VI) heptahydrate (Avantor Performance Materials Poland S.A., Gliwice, Poland) was used to produce the nanoparticles. A solution of chromium(III) nitrate(V) nonahydrate (Honeywell Fluka, Kansas City, Missouri, USA) and ethylenediaminetetraacetic acid (EDTA) (Avantor Performance Materials Poland S.A., Gliwice, Poland) were applied for the sorption process. Hydrochloric acid and sodium hydroxide (Avantor Performance Materials Poland S.A., Gliwice, Poland) were used to adjust the pH of the solutions. EMSURE ACS-grade concentrated HNO_3 (65%, m/v) nitric acid (Merck, KGaA, Darmstadt, Germany) was used for the microwave digestion of samples prior to ICP-OES analysis. Multi-elemental ICP standard solution (1000 mg/L) and single ICP stocks (1000 mg/L) of

P and S (Merck) were used for the calibration of the ICP-OES instrument. Folin–Ciocalteu reagent (Merck), gallic acid (Sigma-Aldrich, Saint Louis, MI, USA), and sodium carbonate (Avantor Performance Materials Poland S.A., Gliwice, Poland) were used to determine the total polyphenol content in the seaweed extract, and the DPPH method was used to measure its antioxidant activity using Trolox, 2,2-diphenyl-1-picrylhydrazyl (Sigma-Aldrich), and methanol (Avantor Performance Materials S.A., Gliwice, Poland).

2.2. The Production of Seaweed Extract and Biosynthesis of ZnO NPs

The brown seaweed *Sargassum* sp. was collected in Vannes (Brittany, France) in February 2019. Before the production of the seaweed extract, the biomass was dried, ground, and subjected to a sieve analysis (400 µm, Retsch, Germany).

The seaweed extract was prepared according to the procedure described by Vaishnav et al. [22]. Accordingly, the dry *Sargassum* biomass (4 g) was suspended in an aqueous solution (80 mL). The ultrasound-assisted extraction (UAE) process of the seaweed was performed using an ultrasonic homogenizer for 30 min (1 cycle) (UP50H/UP100H, Hielscher, Germany). The mixture was then centrifuged at a rate of 4000 rpm for 10 min (Heraeus Megafuge 40 Centrifuge, Thermo Scientific, Waltham, MA, USA). The obtained supernatant was used to biosynthesize ZnO NPs. The *Sargassum* post-extraction residue was dried at 40 °C, ground in a laboratory mortar, and used thereafter as a biosorbent of metal ions.

Zinc oxide nanoparticles were produced according to the methodology described by Vaishnav et al. [22]. Briefly, for the synthesis of ZnO NPs, 100 mL of a 100 mM zinc(II) sulfate(VI) heptahydrate solution was heated to 60 °C in a shaker (250 rpm) with heating (Unimax 1010 Inkubator 1000, Heldolph, Germany) for 30 min. To the heated solution, 15 mL of the extract was added and further shaken for 15 min (250 rpm). Then, the pH was measured with a pH meter (SevenMulti, Mettler-Toledo, Columbus, OH, USA), and 5 M of sodium hydroxide was added to adjust the pH to 12. The solution was shaken (250 rpm) for the next 2 h at 60 °C. The mixture was centrifuged at 4000 rpm for 10 min and then the white precipitate was dried at 70 °C.

2.3. Characteristics of Sargassum Extract

The pH and electrical conductivity (EC) of the seaweed extract were measured using a pH meter with an additional conductivity measurement option (Mettler Toledo Seven-Compact Duo, Columbus, OH, USA). All measurements were performed in duplicate (n = 2).

The standard ISO 14502-1 procedure with the Folin–Ciocalteu reagent was used to determine the total content of phenolic compounds in the seaweed extract. To 0.5 mL of extract, 2.5 mL of the Folin–Ciocalteu reagent was added and mixed. After 4 min, 2.0 mL of a 7.5% (m/v) sodium carbonate solution was added and stirred. After 60 min in the dark, the absorbance was measured using a spectrophotometer (Spectrophotometer Biosens UV 5100, METASH, Warsaw, Poland) at a wavelength of 765 nm. The standard curve was made with gallic acid (GA) (n = 2).

The antioxidant activity of the seaweed extract was measured using the improved Brand-Williams et al. [23] methodology, which included the use of the synthetic radical DPPH. To 0.1 mL of the seaweed extract, 3.9 mL of 0.5 mM alcoholic DPPH solution was added (the absorbance at 515 nm was 0.727). After 30 min in the dark, the absorbance of the sample was measured using a spectrophotometer (Spectrophotometer Biosens UV 5100, METASH, Warsaw, Poland) at a wavelength of 515 nm. The standard curve was made with a 1.5 mM alcoholic Trolox solution (n = 2).

2.4. Characteristics of Zinc Oxide Nanoparticles

A UV–vis spectrophotometer (Genesys 10S UV-VIS Spectro-Lab, Thermo Scientific, Waltham, MA, USA) was used to record the UV absorption spectrum of the ZnO NPs.

An FTIR spectrometer with the ATR attachment (Nicolet 6700, Thermo Scientific, Waltham, MA, USA) was used to identify the functional groups present in the ZnO NPs. The number of scans performed was 32, and the resolution was 4 cm^{-1}.

The X-ray diffraction technique was used for determining the crystallinity of the ZnO NPs [17]. For this purpose, in an agate mortar, about 3 g of ZnO NPs was ground. The sample was tested using a diffractometer X-ray equipped with a PIXcel^{3D} detector (Empyrean, PANalytical, Malvern, UK). The diffractometer working parameters were as follows: voltage 40 kV, current 40 mA, and radiation CuKa λ = 1.5406 Å. The Bragg–Brentano measurement geometry was used, and diffractograms were obtained.

The surfaces of the ZnO NPs were examined using scanning electron microscopy (Quanta 250, FEI). An SE detector was used to assess the surface topography. The samples were gold-sputtered with a thickness of about 10 nm (LEICA EM ACE200).

Before the elemental analysis with ICP-OES, ZnO NPs, as well as the remaining samples (*Sargassum* sp., the *Sargassum* extract, and the *Sargassum* post-extraction residue) were wet-digested. Accordingly, into Teflon vessels, 5.0 g of a liquid sample or 0.25 g of a solid sample was weighed and poured with 5 mL of 65% (m/v) HNO_3. Then, vessels were closed, inserted into a rotor, and digested in a microwave reaction system (Anton Paar GmbH, Graz, Austria) using a 6-stage temperature program. The resulting sample remnants were quantitatively transferred to polypropylene containers (Equimed, Kraków, Poland) and supplemented with deionized water to 25 g. Samples were analyzed in 3 parallel replicates triplicate (n = 3). Simultaneously with digested samples, blanks were prepared and considered in the final results. The measurements were performed with an ICP-OES spectrometer (Dual View 5100, Agilent, Santa Clara, CA, USA) using a 6-point external calibration curve.

2.5. (Bio)Sorption Properties of (Bio)Sorbents

The sorption experiments were carried out on three sorbents: *Sargassum* sp., the *Sargassum* post-extraction residue, and the biosynthesized ZnO NPs. Cr(III) ions were applied as a sorbate since these metal ions are common in wastewater [1–4]. This process was conducted according to the methodology described by Papirio et al. [24] and Michalak and Chojnacka [25], as follows: A solution of Cr(III) ions was prepared via the dissolution of chromium(III) nitrate(V) nonahydrate in water. In order to obtain the appropriate pH of the solution, hydrochloric acid or sodium hydroxide was used. An Erlenmeyer flask contained 0.2 g of sorbent and 200 mL of a previously prepared Cr(III) solution. The solution was placed in a shaker (200 rpm) at room temperature and then the samples were taken and filtered at appropriate time intervals of 5, 10, 15, 20, 25, 30, 45, 60, 90, 120, 150, and 180 min. The sorption process on examined sorbents was carried out for different pH values (3, 4, and 5), different initial concentrations (C_0) of Cr(III) ions (100, 200, and 300 mg/L), and a constant concentration of the sorbent (C_S) in the solution (1.0 g/L). In the tested pH range (3–5), chromium ions exist as $CrOH^{2+}$ ($Cr^{3+} + H_2O \leftrightarrow Cr(OH)^{2+} + H^+$). Above pH 5.5, they precipitate as $Cr(OH)_3$. Therefore, for biosorption experiments, the solution of Cr(III) ions had a pH of 5 or lower [3,25,26].

The concentration of Cr(III) ions in the solution before and after sorption was examined using the spectrophotometric method based on the formation of a violet complex between Cr(III) and EDTA. Therefore, 4.0 mL of the Cr(III)-ion-containing filtrate was mixed with 0.095 g of EDTA. The samples were heated at 95 °C for 10 min and mixed in a stirrer Vortex (Classic Advanced Vortex Mixer, VELP® Scientifica, Usmate Velate, Italy). Then, the absorbance of the samples (violet Cr(III)–EDTA complex) was measured at a wavelength of 540 nm with a spectrophotometer (Spectrophotometer Biosens UV 5100, METASH, Warsaw, Poland).

For the equilibrium studies, solutions of Cr(III) ions at concentrations of 25, 50, 75, 100, 125, 150, 200, 250, and 300 mg/L were prepared. The pH was adjusted to 5 (the value that resulted in the highest biosorption capacity obtained for adsorption kinetics). To 40 mL of each solution, 0.04 g of sorbents (*Sargassum* sp., the *Sargassum* post-extraction residue, and

the biosynthesized ZnO NPs) was added (C_S 1.0 g/L). The mixtures were stirred at 100 rpm at room temperature. After 3 h of stirring (time determined in kinetic experiments), each mixture was filtered through a filter paper. The concentration of Cr(III) ions in the solution before and after sorption was examined using the spectrophotometric method.

Various models were applied to elaborate experimental data from the kinetic and equilibrium studies (Table 1).

Table 1. Kinetic and equilibrium sorption models used in the present study.

Model	Equation	Parameter
		Kinetic model
Pseudo-first-order (PFO)	$q_t = q_{eq}\left(1 - e^{-k_1 \cdot t}\right)$	q_{eq}—sorption capacity at equilibrium (mg/g) q_t—sorption capacity at time t (mg/g) t—time (min) k_1—pseudo-first-order model rate constant (1/min) k_2—pseudo-second-order model rate constant (g/mg·min) k_{ID}—intraparticle diffusion rate constant (mmol/(g·min$^{1/2}$)) C_{WM}—boundary layer thickness
Pseudo-second-order (PSO)	$q_t = \frac{(k_2 \cdot q_{eq} \cdot t)}{1+(k_2 \cdot q_{eq} \cdot t)}$	
Weber–Morris	$q_t = k_{ID} \cdot t^{\frac{1}{2}} + C_{WM}$	
		Isotherm model
Langmuir model	$q_{eq} = q_{max} \cdot \frac{b \cdot C_{eq}}{1+b \cdot C_{eq}}$	q_{eq}—sorption capacity at equilibrium (mg/g) C_{eq}—concentration of metal ions in the solution at equilibrium (mg/L) b—adsorption equilibrium constant (L/mg) q_{max}—maximum sorption capacity (mg/g) n—adsorption intensity K_f—Freundlich isotherm constant (mg$^{(1-1/n)}$ · L$^{1/n}$ · g^{-1}) R—universal gas constant—8.314 J/(mol·K) T—temperature (K) b_t—Temkin isotherm constant A_T—Temkin isotherm equilibrium binding constant (L/g)
Freundlich model	$\log q_{eq} = \left(\frac{1}{n}\right) \cdot \log C_{eq} + \log K_f$	
Temkin mode	$q_{eq} = \frac{RT}{b_T} \cdot \ln\left(A_T C_{eq}\right)$	

The assumptions behind the pseudo-first- and pseudo-second-order models were that the rate of sorption was related to the number of free sites on the sorbent's surface in the proper power. Based on the linearization of these models, the parameters of sorption capacity at equilibrium (q_{eq}) and rate constant (k_1 and k_2, respectively) can be determined (e.g., Martín et al. [27]; Michalak and Chojnacka [25]; Sheela et al. [2]; Cardoso et al. [21]; Mohamed et al. [3]; Gu et al. [4]; and Dziergowska et al. [19]). The Weber–Morris intraparticle diffusion equation may be used to calculate two parameters: the coefficient of intraparticle diffusion and the boundary layer thickness (boundary resistance) [28]. The equation shows that the thickness of the boundary layer has a direct influence on the internal resistance that is associated with the sorption process [21]. Using the Weber–Morris kinetic model, the intraparticle diffusion coefficient and boundary resistance can be calculated (e.g., Bertagnolli et al. [20]; Jha et al. [28]; and Gu et al. [4]).

The Langmuir, Freundlich, and Temkin models were applied to the results from the equilibrium studies. The Langmuir adsorption isotherm assumes monolayer adsorption on the surface of the sorbent and enables the determination of the maximum sorption capacity (q_{max}) (e.g., Dada et al. [29]; Jin et al. [30]; and Mohamed et al. [3]). The Freundlich adsorption isotherm is used to describe the adsorption characteristics of the heterogeneous surface and multilayer adsorption (e.g., Dada et al. [29]; Jin et al. [30]; and Mohamed et al. [3]). An n-value in the Freundlich model greater than 1 indicates favorable adsorption of metal ions on the surface of the adsorbent [3,6,7]. The Temkin isotherm includes a factor that explicitly accounts for adsorbent–adsorbate interactions. The model ignores the extremely low and large values of concentrations and assumes that the heat of adsorption (function of temperature) of all molecules in the layer would decrease linearly and not logarithmically with coverage [3,29].

3. Results and Discussion

3.1. Characteristics of Sargassum Extract

The *Sargassum* sp. extract obtained with UAE had a pH of 6.05 ± 0.02 and EC of 18.1 ± 0.2 mS/cm. The resulting extract was slightly acidic. The total concentration of polyphenols in the extract was 146 ± 11 mg GA/L. The total antioxidant activity was 0.773 ± 0.026 mmol Trolox/L, and the inhibition percentage was 35.4 ± 2.02%. In all seaweeds, phenols and polyphenols are abundant active compounds that are recognized as powerful antioxidants, not just for their ability to donate electrons or hydrogen atoms, but also for the stable radical intermediates they produce [31]. These compounds play an important role in the biosynthesis of nanoparticles. Elrefaey et al. [18] indicated that phenolic compounds and proteins present in the extract from brown marine alga *Cystoseira crinita* (*Sargassaceae*) acted as reducing, capping, and stabilizing agents in the biosynthesis of ZnO NPs.

3.2. Characteristics of Zinc Oxide Nanoparticles

The UV–Vis, FTIR, XRD, SEM, and ICP-OES techniques were used to characterize the *Sargassum* sp.-fabricated ZnO NPs. These analyses provide important information on the physicochemical properties of synthesized nanostructures.

During the biosynthesis of ZnO NPs, the color of the solution (a mixture of zinc solution and the seaweed extract) changed, indicating the formation of nanoparticles. The used algal extract was brown at first, but after combining it with a colorless solution of zinc sulfate(VI), a cloudy-white solution was observed (Figure 1). The same phenomenon was observed by Azizi et al. [15], who produced ZnO NPs using *Sargassum muticum* aqueous extract and dehydrated zinc acetate as a precursor of zinc ions. The UV–Vis absorption spectrum of the ZnO NPs revealed absorption peaks in the UV region, which were attributed to the ZnO NPs. In the present study, two characteristic peaks at 269 and 366 nm were noticed, indicating the formation of ZnO NPs (Figure 1). According to various publications, the existence of a peak between 230 and 390 nm indicates the development of ZnO NPs [6,15,18,19]. According to Azizi et al. [6] a typical absorption peak of ZnO NPs appears at a wavelength of 353 nm.

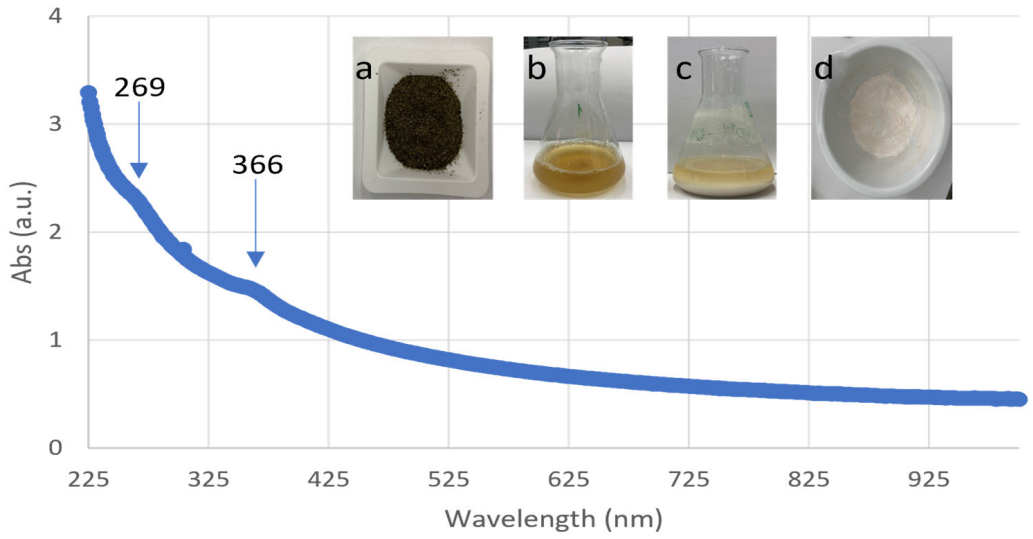

Figure 1. UV–vis spectrum of ZnO NPs synthesized with *Sargassum* sp.: (**a**) macroalgae *Sargassum* sp. after sieve analysis, (**b**) aqueous extract from *Sargassum* sp., (**c**) biosynthesized ZnO NPs, and (**d**) ZnO NPs after drying.

FTIR is a useful technique for the identification of molecules in which functional groups are responsible for the reduction of metal ions and are acting as a capping agent in nanoparticle biosynthesis [16,18]. The FTIR spectrum of the biosynthesized ZnO NPs

is presented in Figure 2. A wide band at 3382 cm^{-1} could be attributed to the stretching vibrations of OH groups. The band at 1616 cm^{-1} could be assigned to the stretching vibrations of (NH) C=O groups, which are characteristic of proteins. The bands present at wavelengths 1406 and 1105 cm^{-1} may be due to bending vibrations in the C-O-H. The peak at 623 cm^{-1} indicates the band derived from the metal oxide (Zn–O bonds).

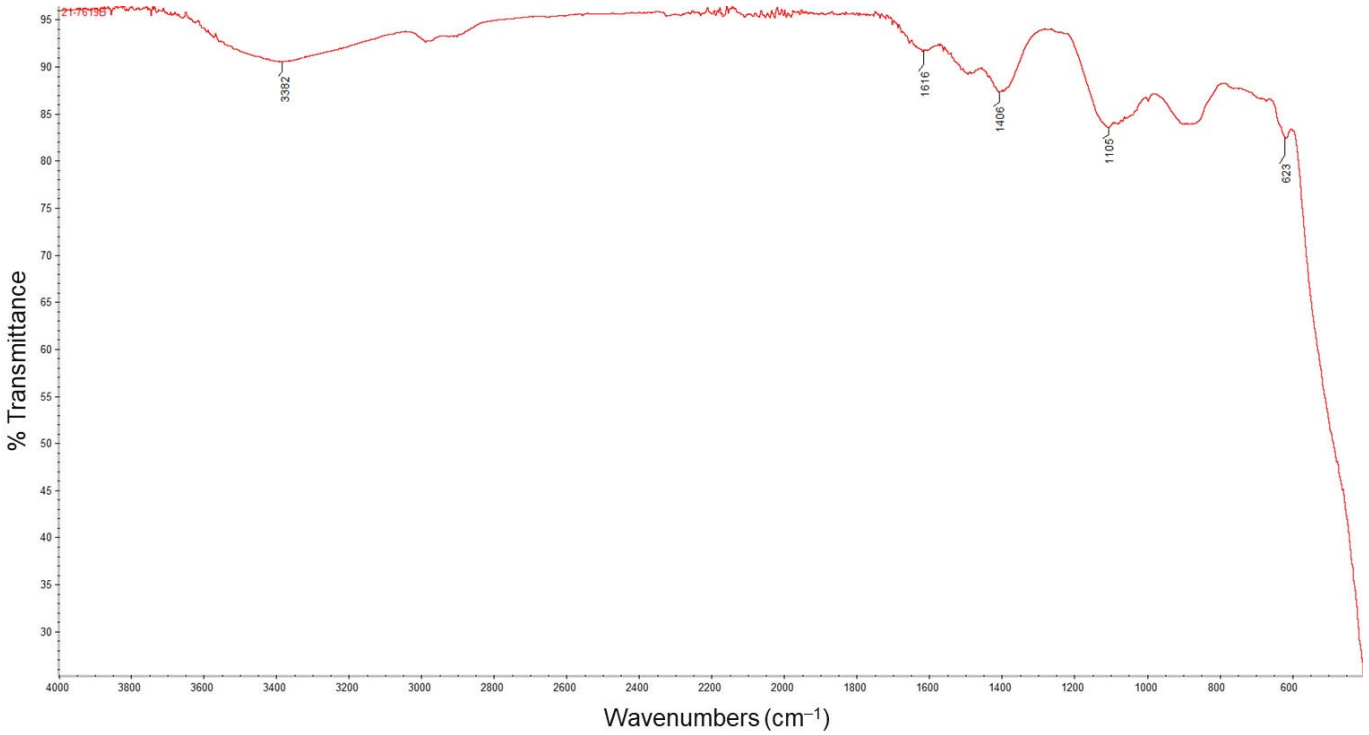

Figure 2. FTIR spectrum of the biosynthesized ZnO NPs.

Similar results were obtained by Elrefaey et al. [18] for ZnO NPs produced with the use of an extract from brown seaweed *Cystoseira crinita*, whereby the following peaks were detected: 3257, 1590, 1382, 1036, 693, 598, and 520 cm^{-1}. The OH stretching H-bonded alcohols and phenols were responsible for the peak at 3257 cm^{-1}. The band at 1590 cm^{-1} was attributed to the stretching vibration of the (NH) C=O group and at 1382 cm^{-1} to the CH-aliphatic. A band at 1036 cm^{-1} was assigned to the C-N stretching vibrations of aromatic and aliphatic amines. The peaks lower than 1000 cm^{-1} were attributed to the characteristic absorption peaks of the Zn–O bond [18]. Based on FTIR spectra, Azizi et al. [15] showed that the sulfate and hydroxyl groups of the *Sargassum muticum* polysaccharide participated in the formation of ZnO NPs. The signal at 1235 cm^{-1} in raw seaweed, which is attributed to the asymmetric stretching vibration of a sulfate group, disappeared after the synthesis of ZnO NPs.

ZnO NPs produced using the traditional hydrothermal method also presented a similar spectrum. The absorption peaks at 3403 cm^{-1} supported the O–H stretching vibration and the bands at 1643 cm^{-1} and 1383 cm^{-1} corresponded to the bending mode of H_2O, which originated from adsorption in the air. Some absorption bands at 428 cm^{-1} and 568 cm^{-1} belonged to the stretching vibrations of Zn–O bonds [4]. According to Azizi et al. [15], the formation of ZnO NPs was clearly confirmed by an intense band at 410 cm^{-1}.

The XRD pattern of the biosynthesized ZnO NPs is presented in Figure 3.

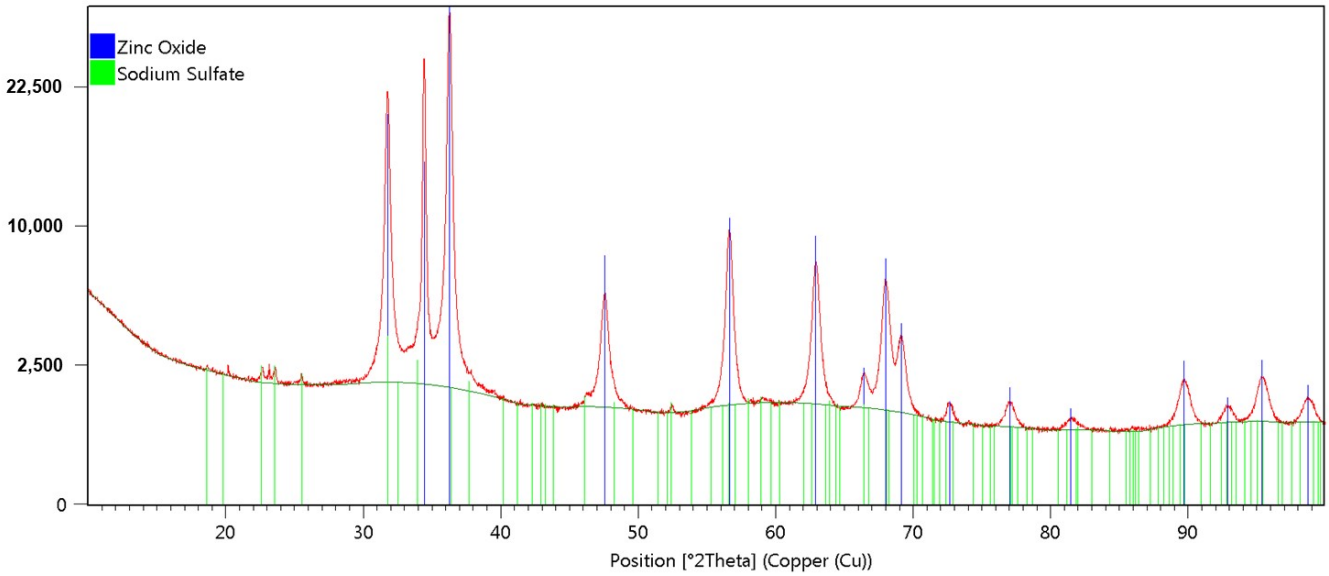

Figure 3. XRD pattern of the biosynthesized ZnO NPs.

The biosynthesized ZnO NPs showed characteristics peaks at 2θ values of about 31.75°, 34.41°, 36.25°, 47.53°, 56.59°, 62.88°, and 67.96° on the XRD pattern, which were assigned to the (1 0 0), (0 0 2), (1 0 1), (1 0 2), (1 1 0), (1 0 3), and (1 1 2) planes. Our results are in accordance with numerous studies that have reported similar XRD patterns of phyco-synthesized ZnO NPs. All of the recorded peak intensity profiles were typical of the nanoparticles' hexagonal wurtzite structure, indicating that the ZnO NPs were well crystallized. The same structure of ZnO NPs was obtained by Azizi et al. [15] and Elrefaey et al. [18], who used extracts from marine brown macroalgae *Sargassum muticum* and *Cystoseira crinita* for their biosyntheses, respectively.

The diffraction peaks for ZnO NPs synthesized biologically are also comparable to the diffraction peaks for ZnO NPs synthesized hydrothermally or chemically. This proves that environmentally friendly methods can produce nanoparticles with the same structure produced using physical/chemical methods. Zinc oxide nanoparticles synthesized with the traditional hydrothermal method (at 110 °C for 5 h) showed diffraction angles (2θ) at 31.62°, 34.34°, 36.23°, 47.63°, 56.64°, 62.94°, and 67.91°, which could be indexed as (1 0 0), (0 0 2), (1 0 1), (1 0 2), (1 1 0), (1 0 3), and (1 1 2) crystal planes, in accordance with the standard data on hexagonal ZnO crystal structures [4]. Major diffraction peaks for ZnO NPs synthesized chemically (from $ZnSO_4 \cdot 7H_2O$ and cetyl trimethylammonium bromide) were seen at 31.96°, 34.62°, 36.44°, 47.74°, 56.79°, and 63.05°, which can be assigned to diffraction from the (1 0 0), (0 0 2), (1 0 1), (1 0 2), (1 1 0) and (1 0 3) planes, respectively [2]. This revealed that the produced nanoparticles were pure zinc oxide with a hexagonal structure. The crystallinity of the product was indicated by the strong and narrow diffraction peaks [2,5].

Scanning electron microscopy (SEM) was used to visualize the surfaces of the ZnO NPs produced from the *Sargassum* sp. extract (Figure 4). The SEM analysis revealed the surface morphology and the shape of the biosynthesized nanoparticles. They have a snowflake-like morphology, similar to that described by Dziergowska et al. [19] for ZnO NPs produced from green macroalga (*Cladophora glomerata*). Additionally, it can be seen that aggregates/agglomerates have been formed between the NPs, which may be responsible for the different sizes of the NPs. A spherical shape and highly porous structure were exhibited by ZnO NPs obtained using a hydrothermal method [4] and chemical method [2]. The highly porous structure of nanoparticles may play a key role in the sorption of metal ions.

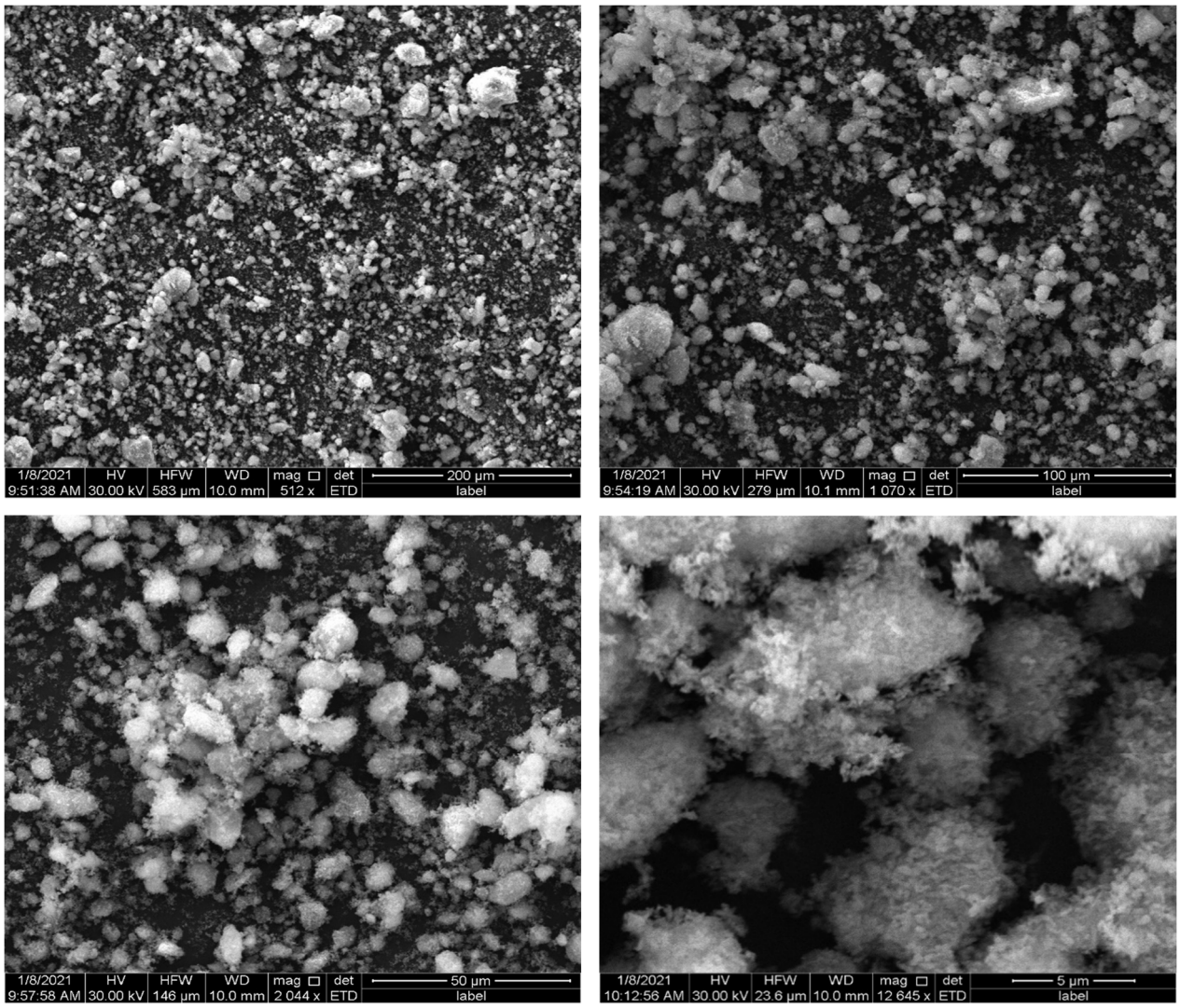

Figure 4. SEM images of biosynthesized ZnO NPs.

An analysis of the elemental compositions of the raw seaweed *Sargassum* sp., the *Sargassum* sp. extract, the post-extraction residue, and the biosynthesized ZnO NPs is presented in Table 2. It must be commented that the multielement composition of synthesized nanoparticles is randomly studied. In this study, it was shown that the ZnO NPs contained the highest amounts of Zn, S, and Na due to the reagents used for their synthesis. Some micro- and macro-elements can be derived from the seaweed extract. The content of Zn in ZnO NPs produced from green seaweed (*Cladophora glomerata*) using the same methodology was almost 700,000 mg/kg d.m. in [19], which may suggest that the species of algae and the volume of the extract used for biosynthesis affect the content of this element in nanoparticles.

3.3. Sorption Properties of Different Sorbents towards Cr(III) Ions

In the present study, the sorption properties of different (bio)sorbents towards Cr(III) ions were compared (raw *Sargassum* sp., the *Sargassum* sp. post-extraction residue, and ZnO NPs). Kinetic models (pseudo-first-order and pseudo-second-order models, and the intra-particle diffusion model) were used to investigate the mechanism of sorption of metal ions and to determine the rate-controlling step of metal ion adsorption onto (bio)sorbents. The sorption kinetics also aimed at determining the time necessary to achieve equilibrium. For the best sorption conditions, i.e., C_0 300 mg/L, C_S 1.0 g/L, and pH 5.0, the values of the

sorption capacity at equilibrium and the rates for PSO and PFO, as well as the parameters in the Weber–Morris equation, were calculated and are presented in Table 3.

Table 2. Elemental compositions of *Sargassum* sp. and *Sargassum* sp.-derived bioproducts (*Sargassum* sp. extract, *Sargassum* sp. post-extraction residue, and ZnO NPs; $n = 3$).

Element	*Sargassum* sp. (mg/kg d.m.)	*Sargassum* sp. Extract (mg/L)	*Sargassum* sp. Post-Extraction Residue (mg/kg d.m.)	ZnO NPs (mg/kg d.m.)
Al	2308 ± 57	6.93 ± 0.06	2487 ± 58	329 ± 2
B	71.6 ± 1.7	2.44 ± 0.01	48.8 ± 0.1	72.5 ± 0.2
Ca	18,763 ± 631	71.2 ± 0.6	21,816 ± 125	890 ± 21
Cd	1.56 ± 0.03	0.007 ± 0.001	2.30 ± 0.03	0.990 ± 0.010
Cr	3.71 ± 0.12	0.040 ± 0.002	6.19 ± 0.31	7.27 ± 0.26
Cu	4.15 ± 0.11	0.019 ± 0.001	9.23 ± 0.40	3.55 ± 0.08
Fe	2468 ± 187	4.56 ± 0.02	2555 ± 65	75.9 ± 1.0
K	66,244 ± 1559	2955 ± 8	27,881 ± 171	3396 ± 31
Mg	25,002 ± 453	861 ± 1	16,618 ± 144	11,557 ± 56
Mn	174 ± 8	3.86 ± 0.01	165 ± 1	51.3 ± 0.4
Na	9353 ± 132	422 ± 3	3800 ± 36	40,088 ± 179
P	4100 ± 101	165 ± 1	2363 ± 22	2074 ± 12
S	13,629 ± 142	407 ± 4	11,970 ± 185	29,650 ± 40
Zn	27.2 ± 0.6	0.231 ± 0.020	22.9 ± 1.1	578,013 ± 6888

d.m.—dry mass.

Table 3. Calculated parameters of kinetic models for the tested sorbents under conditions C_0 300 mg/L, C_S 1.0 g/L, and pH 5.0.

Model	*Sargassum* sp.	*Sargassum* sp. Post-Extraction Residue	ZnO NPs
Pseudo-first-order (PFO)	q_{eq1} = 10.4 mg/g k_1 = 0.00964 1/min R^2 = 0.624	q_{eq1} = 49.7 mg/g k_1 = 0.0193 1/min R^2 = 0.889	q_{eq1} = 56.4 mg/g k_1 = 0.0164 1/min R^2 = 0.860
Pseudo-second-order (PSO)	q_{eq2} = 82.0 mg/g k_2 = 0.00315 g/mg·min R^2 = 0.996	q_{eq2} = 81.3 mg/g k_2 = 0.000932 g/mg·min R^2 = 0.985	q_{eq2} = 137 mg/g k_2 = 0.000862 g/mg·min R^2 = 0.996
Weber–Morris	C_{WM} = 1.29 k_{ID} = 0.0226 mmol/(g·min$^{1/2}$) R^2 = 0.714	C_{WM} = 0.367 k_{ID} = 0.0951 mmol/(g·min$^{1/2}$) R^2 = 0.790	C_{WM} = 1.50 k_{ID} = 0.0847 mmol/(g·min$^{1/2}$) R^2 = 0.939

The highest determination coefficients (above 0.980) were obtained for all sorbents with the pseudo-second-order model, which was further used in this study. Moreover, this model is commonly used to describe the sorption of Cr(III) ions by different sorbents, e.g., brown seaweeds *Macrocystis pyrifera* and *Undaria pinnatifida* [26], green seaweeds *Enteromorpha prolifera* [25] and *Cladophora glomerata* [19], the residue after alginate extraction from *Sargassum filipendula* [20], zinc oxide nanoparticles synthesized with the traditional hydrothermal method [4], etc. The pseudo-second-order model implies chemisorption involving covalent forces as well as ion exchange [4].

The effects of different pH values and initial concentrations of metal ions in the solution on the sorption capacity at equilibrium (q_{eq}) and the constant rate (k_2) determined with the pseudo-second-order model are presented in Table 4 and Figure 5 (for pH) and Figure 6 (for C_0).

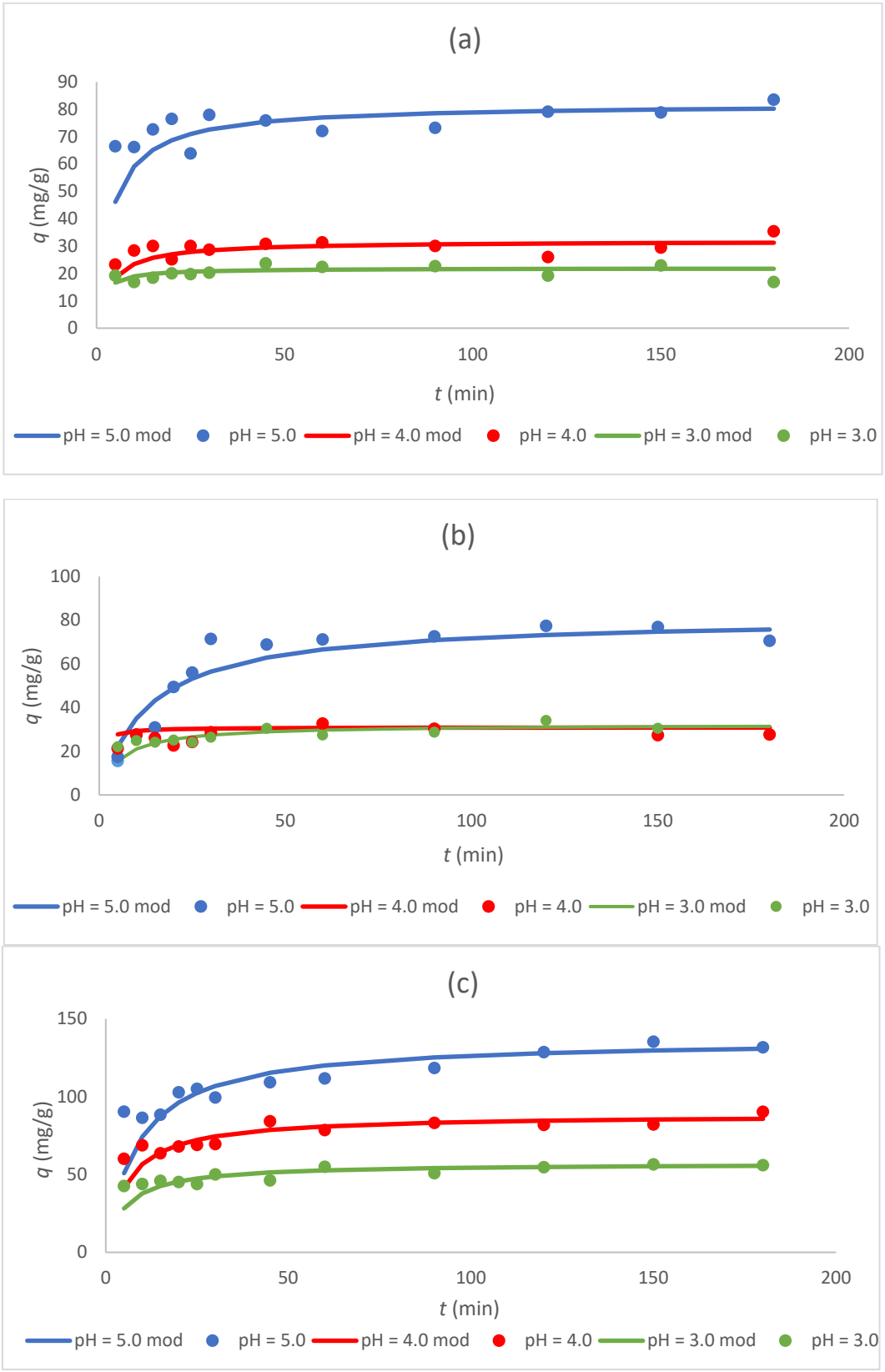

Figure 5. Dependence of the sorption capacity of the tested sorbents (**a**) *Sargassum* sp., (**b**) *Sargassum* sp. post-extraction residue, and (**c**) ZnO NPs on time for different pH values (3, 4, and 5; "mod"—model) at C_0 300 mg/L and C_S 1.0 g/L.

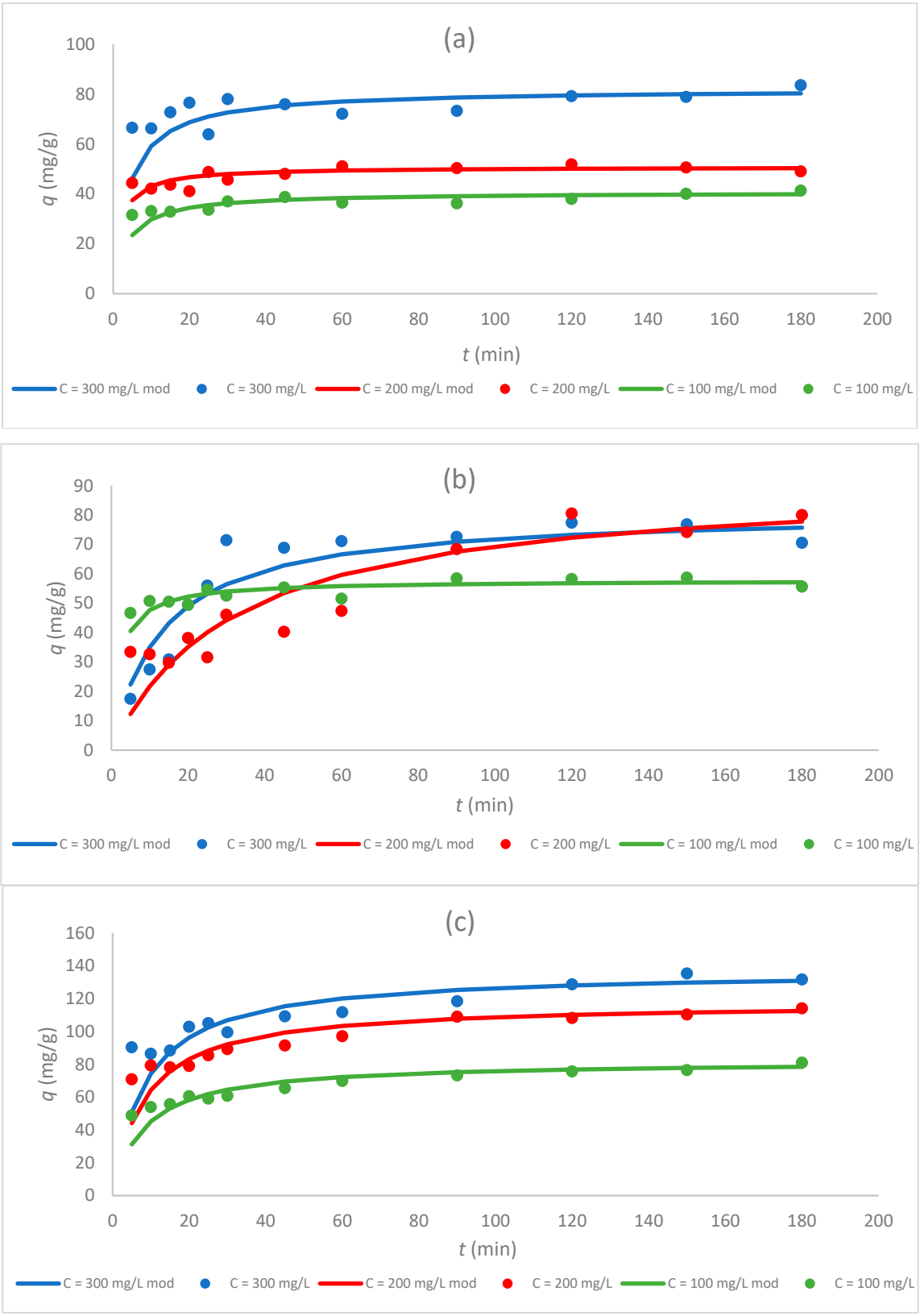

Figure 6. Dependence of the sorption capacity of the tested sorbents (**a**) *Sargassum* sp., (**b**) *Sargassum* sp. post-extraction residue, and (**c**) ZnO NPs on time for different initial concentrations of Cr(III) ions (100, 200, and 300 mg/L) at pH 5 and C_S 1.0 g/L.

Table 4. Comparison of the parameters of the pseudo-second-order model at different pH (C_0 300 mg/L, C_S 1.0 g/L) and C_0 (pH 5, C_S 1.0 g/L) values for the tested sorbents.

Parameter	*Sargassum* sp.			*Sargassum* sp. Post-Extraction Residue			ZnO NPs		
	q_{eq2} (mg/g)	k_2 (g/mg·min)	R^2	q_{eq2} (mg/g)	k_2 (g/mg·min)	R^2	q_{eq2} (mg/g)	k_2 (g/mg·min)	R^2
				pH					
3	21.9	0.0289	0.985	32.4	0.00571	0.990	57.1	0.00340	0.997
4	31.9	0.00873	0.971	31.0	0.0564	0.950	88.5	0.00200	0.995
5	82.0	0.00315	0.996	81.3	0.000932	0.985	137	0.000862	0.996
				C_0 (mg/L)					
100	40.7	0.00672	0.996	57.8	0.00811	0.998	82.0	0.00150	0.997
200	50.8	0.0111	0.998	91.7	0.000338	0.939	117	0.00102	0.998
300	82.0	0.00315	0.996	81.3	0.000932	0.985	137	0.000862	0.996

Figures 5 and 6 show that the sorption capacity increased rapidly with an increasing contact time at first, and then reached equilibrium after 50 min. Furthermore, once equilibrium was reached, the adsorption capacity for Cr(III) ions became constant for all tested sorbents. These data coincide with the results obtained in other studies in which biologically synthesized ZnO NPs were used for the sorption of Pb(II) ions [15] or chemically synthesized ZnO NPs for the sorption of Cr(VI) ions [5].

3.4. Effect of pH on the Sorption Process

The highest sorption capacity at equilibrium for all tested sorbents was achieved at pH 5 (Table 4, Figure 5). At pH 4, the sorption capacity of the biosorbents was approximately 2.5 times lower than at pH 5 and for ZnO NPs, about 1.5 times lower. The lowest sorption capacity for all sorbents was obtained at pH 3. The highest value of the sorption capacity was calculated for ZnO NPs at pH 5 (137 mg/g) and was ~67% higher than that for tested biosorbents, *Sargassum* sp., and the *Sargassum* sp. post-extraction residue, which demonstrated similar sorption properties in the tested pH range. Because chromium ions were present as cations in the studied pH values, the reduced adsorption capacity at low pH values can be described by the competition of chromium ions with protons for adsorption sites, as well as the electrostatic repulsion between the protonated biomass surface and metal cations [27]. Bertagnolli et al. [20] also investigated the biosorption of Cr(III) ions via the post-extraction residue (alkaline alginate extraction) of *Sargassum filipendula*, and the value of sorption capacity at equilibrium was 20.7 mg/g for pH 3 and C_S 2.0 g/L. This value was lower than that obtained in the present study for pH 3, but the initial concentration of the tested Cr(III) ions was only 52 mg/L. However, it was shown that the post-extraction residue can be utilized as a suitable, easily available, and cheap biosorbent for chromium uptake [20]. The sorption capacities of seaweed *Sargassum* and the *Sargassum* sp. post-extraction residue was similar, which may indicate comparable sorbent characteristics and a related binding mechanism of Cr(III) ions.

For ZnO NPs produced from the *Sargassum* extract, the highest value of sorption capacity was obtained among the tested sorbents (137 mg/g at pH 5). The sorption capacity of ZnO NPs at pH 3 was 57.1 mg/g, and it was 58.3% lower than the value calculated for pH 5. In the study of Gu et al. [4], the sorption capacity of ZnO NPs synthesized using the traditional hydrothermal method towards Cr(III) ions increased sharply with an increase in pH from 2 to 3, and then began to decrease slightly with an increase in pH from 3 to 7. It was concluded that ZnO NPs can effectively remove Cr(III) ions at a pH above 3 [4].

3.5. Effect of the Initial Concentration of Cr(III) Ions on the Sorption Process

Concentrations of 100, 200, and 300 mg/L of Cr(III) ions were used to investigate the effect of the initial concentration of metal ions on the sorption properties of sorbents. This experiment was performed for a constant pH equal to 5 and a C_S of 1.0 g/L. The change

in the sorption capacity during the sorption for different sorbents is compared in Figure 6 and Table 4. The highest values of the sorption capacity were obtained for a C_0 equal to 300 mg/L for seaweed *Sargassum* sp. (82.0 mg/g) and zinc oxide nanoparticles (137 mg/g), and this parameter increased with the increase in the initial concentration of Cr(III) ions. The same relationship was observed for the sorption of Cr(III) ions by other sorbents, which has been tested in the literature, e.g., green seaweed (*Enteromorpha prolifera*) [25] or ZnO NPs synthesized hydrothermally [4]. For *Sargassum* sp., the sorption capacity at C_0 300 mg/L was about twice that of the initial concentration of 100 mg/L (40.7 mg/g). For ZnO NPs, the sorption capacity for C_0 300 mg/L was about 1.5 times higher than the sorption capacity for 100 mg/L. The increase in the sorption capacity with the increasing initial metal ion concentration can be due to an increase in the driving force caused by the concentration gradient formed between the bulk solution and the surface of the sorbent. At higher metal ion concentrations, the active sites of sorbents can be surrounded by much more metal ions, and the adsorption process continues, resulting in an increased metal ion uptake from the solution [2].

For the *Sargassum* post-extraction residue, the highest value of the sorption capacity was gained for the initial concentration of Cr(III) ions equal to 200 mg/L (91.7 mg/g), while the lowest was received for the post-extraction residue at a concentration of 100 mg/L (a 37% decrease). At the highest initial concentration (300 mg/L), the value of q_{eq} was equal to 81.3 mg/g and was lower by 10.4 mg/g than the highest value of capacity for this sorbent. The same phenomenon was observed in the work of Dziergowska et al. [19], in which among the tested concentrations (100, 200, and 300 mg/L), the highest value of the sorption capacity for the *Cladophora glomerata* post-extraction residue was obtained at a concentration of 200 mg/L.

Table 5 compares the sorption capacities of *Sargassum* sp. and ZnO NPs, produced using chemical and biological methods, determined from kinetic models in relation to various metal ions. Considering the initial concentration of Cr(III) ions in the solution, the ZnO NPs were very effective at binding these ions this study, [4,19].

Table 5. Comparison of the values of sorption capacities determined on the basis of kinetic models depending on the sorption conditions, metal ion, and sorbent used.

Sorbent	Metal Ion	Sorption Conditions	Sorption Capacity	Reference
***Sargassum* sp. as a biosorbent of metal ions**				
Sargassum filipendula	Pb(II)	pH 4, 30 °C, C_0 47.7 mg/L, C_S 2.0 g/L	280 mg/g	[8]
Sargassum vulgare	Fe(III)	pH 2, 25 °C, C_0 100 mg/L, C_S 5.0 g/L	14.3 mg/g	[9]
Sargassum thunbergii	Cr(VI)	pH 2, 45 °C, C_0 104 mg/L, C_S 1.0 g/L	96.7 mg/g	[14]
Sargassum sp.	Cr(III)	pH 5, RT, C_0 300 mg/L, C_S 1.0 g/L	82.0 mg/g	This study
ZnO NPs as a sorbent of metal ions				
ZnO NPs (*Zingiber zerumbet*) *	Pb(II)	pH 5, 70 °C, C_0 10 mg/L, C_S 0.1 g/L	2.10 mg/g	[6]
ZnO NPs (*Peganum harmala*) *	Cr(VI)	pH 2, 50 °C, C_0 50 mg/L, C_S 2.0 g/L	24.4 mg/g	[32]
ZnO NPs (chemical method)	Cr(III)	pH 3–7, C_0 20 mg/L, C_S 1.0 g/L	19.9 mg/g	[4]
ZnO NPs (*Cladophora glomerata*) *	Cr(III)	pH 4, RT, C_0 300 mg/L, C_S 1.0 g/L	227 mg/g	[19]
ZnO NPs (*Sargassum* sp.) *	Cr(III)	pH 5, RT, C_0 300 mg/L, C_S 1.0 g/L	137 mg/g	This study

where RT—room temperature; * biomass used to produce an extract for the biosynthesis of nanoparticles.

3.6. Sorption Equilibrium

Adsorption isotherms are essential for analyzing the mechanism of sorption of metal ions by (bio)sorbents. The results obtained in the equilibrium experiments were fitted to the Langmuir, Freundlich, and Temkin isotherms, and the obtained results are presented in Table 6.

Table 6. Calculated parameters of isotherm models for the tested sorbents under the selected conditions: C_0 25–300 mg/L, C_S 1.0 g/L, and pH 5.0.

Model	*Sargassum* sp.	*Sargassum* sp. Post-Extraction Residue	ZnO NPs
Langmuir model	q_{max} = 59.9 mg/g b = 0.0389 L/mg R^2 = 0.924	q_{max} = 66.7 mg/g b = 0.123 L/mg R^2 = 0.988	q_{max} = 120 mg/g b = 1.84 L/mg R^2 = 0.776
Freundlich model	K_f = 11.6 $mg^{(1-1/n)} \cdot L^{1/n} \cdot g^{-1}$ n = 3.51 R^2 = 0.580	K_f = 15.9 $mg^{(1-1/n)} \cdot L^{1/n} \cdot g^{-1}$ n = 3.38 R^2 = 0.919	K_f = 77.9 $mg^{(1-1/n)} \cdot L^{1/n} \cdot g^{-1}$ n = 8.75 R^2 = 0.835
Temkin model	A_T = 1.90 L/mg b_T = 293 B = 8.41 J/mol R^2 = 0.555	A_T = 1.76 L/mg b_T = 204 B = 12.1 J/mol R^2 = 0.947	A_T = 532 L/mg b_T = 204 B = 12.1 J/mol R^2 = 0.775

Generally, the highest values of the coefficient of determination for all sorbents were obtained with Langmuir model. Moreover, this model is the most often used in the literature for the description of the sorption of heavy metal ions [19,21,29,30,33]. The best fit of the experimental data with the Langmuir isotherm model suggests a chemisorption procedure and monolayer-type removal [2,4]. Gu et al. [6] also confirmed that the Langmuir model (among the tested Freundlich and Temkin models) was considered the most appropriate for the description of Cr(III) ion adsorption onto ZnO NPs, assuming that their removal occurred on a homogeneous monolayer with uniform active sites, with an equivalent adsorption energy, and without interactions between the adsorbed species. The same conclusions were made by Sheela et al. [2] for the sorption of Zn(II), Cd(II), and Hg(II) ions by ZnO NPs. The Langmuir isotherms for the examined (bio)sorbents are presented in Figure 7.

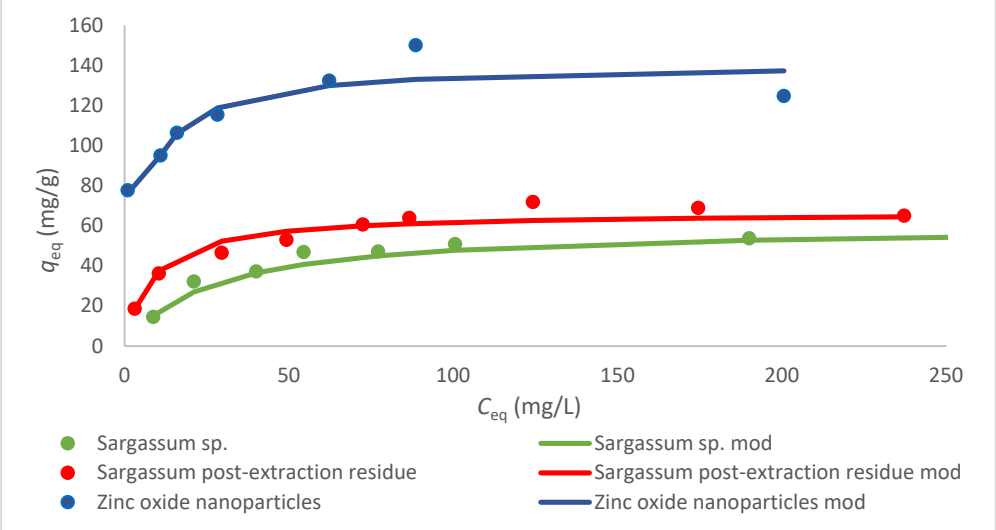

Figure 7. Langmuir isotherms for different sorbents (C_0 25–300 mg/L, C_S 1.0 g/L, and pH 5).

From all the sorbents examined in this study, the highest value of q_{max} was obtained for ZnO NPs (120 mg/g), then for the *Sargassum* sp. post-extraction residue, and finally for *Sargassum* sp. These results coincide with the outcomes obtained for the kinetics of the sorption process. A comparison of the maximum sorption capacities of the tested sorbents towards Cr(III) ions with the results obtained by different researchers is difficult because the process is usually performed under different experimental conditions (Table 7).

Table 7. Comparison of the values of maximum sorption capacities determined on the basis of equilibrium sorption models depending on the sorption conditions, metal ion, and sorbent used.

Sorbent	Metal Ion	Sorption Conditions	q_{max}	Reference
***Sargassum* sp. as a biosorbent of metal ions**				
Sargassum sp.	Ni(II)	pH 5, 30 °C, C_0 0–411 mg/L, C_S 1.3 g/L	53.6 mg/g	[10]
Sargassum sp.	Cr(III)	pH 4, 30 °C, C_0 10–300 mg/L, C_S 1.0 g/L	68.9 mg/g	[11]
Sargassum sp.	Cr(III)	pH 3.5, 30 °C, C_0 104–624 mg/L, C_S 1.2 g/L	68.2 mg/g	[12]
Sargassum sp.	Cu(II)	pH 5, 30 °C, C_0 0–445 mg/L, C_S 1.3 g/L	94.1 mg/g	[10]
Sargassum wightii	Cr(III)	pH 5, RT, C_0 50–200 mg/L, C_S 25 g/L	79.6 mg/g	[13]
Sargassum sp.	Cr(III)	pH 5, RT, C_0 25–300 mg/L, C_S 1.0 g/L	59.9 mg/g	This study
ZnO NPs as a sorbent of metal ions				
ZnO NPs (chemical method)	Cr(III)	pH 3–7, C_0 10–100 mg/L, C_S 1.0 g/L	88.6 mg/g	[4]
ZnO NPs (chemical method)	Zn(II)	pH 5.5, C_0 100–600 mg/L, C_S 0.0005 g/L	357 mg/g	[2]
ZnO NPs (chemical method)	Cd(II)	pH 5.5, C_0 100–600 mg/L, C_S 0.0005 g/L	384 mg/g	[2]
ZnO NPs (chemical method)	Hg(II)	pH 5.5, C_0 100–600 mg/L, C_S 0.0005 g/L	714 mg/g	[3]
ZnO NPs (*Cladophora glomerata*) *	Cr(III)	pH 4, RT, C_0 25–300 mg/L, C_S 1.0 g/L	57.0 mg/g	[19]
ZnO NPs (*Sargassum* sp.) *	Cr(III)	pH 5, RT, C_0 25–300 mg/L, C_S 1.0 g/L	120 mg/g	This study

where RT—room temperature; * biomass used to produce an extract for the biosynthesis of nanoparticles.

Based on Table 7, it can be concluded that ZnO NPs show very good sorption properties in relation to various heavy metal ions. ZnO NPs obtained from the *Sargassum* sp. extract had a higher capacity in relation to Cr(III) ions than the nanoparticles biosynthesized from the *Cladophora glomerata* extract, for similar experimental conditions; the only difference was in pH (which was higher in the present study), which, however, has a significant impact on the sorption capacity. For *Sargassum* sp., the values of q_{max} in relation to different metal ions are comparable for given experimental conditions. Up to this day, only a few algal post-extraction residues have been used as biosorbents of heavy metal ions (mostly after polysaccharide (alginate or agar) extraction but also after oil extraction). However, there is no other research work on the ability of the *Sargassum* sp. residue obtained during ultrasound-assisted extraction to adsorb Cr(III) ions. Similar conditions of the equilibrium process (C_S 1.0 g/L and C_0 25–300 mg/L), but with a lower pH (4 instead of 5), were applied for the *Cladophora glomerata* post-extraction residue after UAE. The obtained value of q_{max} was higher (192 mg/g) [19] than that for the *Sargassum* sp. residue (66.7 mg/g).

The mechanism of Cr(III) ion sorption by the tested sorbents may vary. Due to the fact that brown seaweeds contain mainly cellulose, alginic acids, and polysaccharides in the cell wall, mechanisms such as ion exchange, electrostatic interaction, and complex formation may occur [33,34]. Both sorbents contained light metal ions in the biomass, especially Ca, K, and Mg (Table 2), which can participate in ion exchange, which is considered a dominating mechanism of sorption by biosorbents [3,16,21,25].

Taking into account the mechanism of metal ion sorption by ZnO NPs, it is supposed that the surface of a metal oxide in an aqueous solution is hydroxylated via the dissociative chemisorption of water molecules. The theory of hard and soft acids and bases defines the interaction between heavy metal ions and hydroxyl groups. The hydroxy group is a hard base ligand, and it has a high affinity when it interacts with a hard Lewis ligand (Cr(III) ions) [4]. According to Sheela et al. [2], metal ions may initially move through the pores of ZnO NPs or through crystal lattice channels during the possible ion exchange process.

4. Conclusions

In the present study, ZnO NPs were synthesized via a biological method with *Sargassum* extract and characterized with UV–vis, FTIR, XRD, SEM, and ICP-OES techniques. The sorption capacity of ZnO NPs towards Cr(III) ions was compared with *Sargassum* sp. biomass as well as the *Sargassum* sp. post-extraction residue. The adsorption experiments were conducted under varying experimental conditions such as solution pH and initial

concentration of Cr(III) ions. The pseudo-second-order model and Langmuir isotherm were the most appropriate for describing sorption kinetics and equilibrium. Our results revealed that ZnO NPs showed the highest maximum sorption capacity towards Cr(III) ions among the tested sorbents at pH 5 and C_0 300 mg of Cr(III) ions/L, which was equal to 120 mg/g. ZnO NPs could offer an effective method for removing toxic heavy metals from wastewater, as was shown in this work.

Author Contributions: Conceptualization, N.N. and I.M.; methodology, N.N., M.W., A.S.-M. and I.M.; software, N.N. and K.D.; validation, M.W. and A.S.-M.; formal analysis, N.N., K.D. and I.M.; investigation, N.N., K.D., M.W., A.S.-M. and J.C.; resources, M.W., A.S.-M., J.C. and N.B.; data curation, N.N., K.D. and I.M.; writing—original draft preparation, N.N., K.D. and I.M.; writing—review and editing, I.M., M.W. and A.S.-M.; visualization, N.N.; supervision, I.M.; project administration, I.M.; funding acquisition, I.M. All authors have read and agreed to the published version of the manuscript.

Funding: This research was funded by the National Science Centre in Poland, grant number 2019/33/B/NZ9/01844, titled "Eco-friendly technologies for the management of seaweed biomass for products useful for sustainable agriculture and biosorbents used for the removal of heavy metal ions from the environment".

Data Availability Statement: Not applicable.

Conflicts of Interest: The authors declare no conflict of interest.

References

1. Jaishankar, M.; Tseten, T.; Anbalagan, N.; Mathew, B.B.; Beeregowda, K.N. Toxicity, mechanism and health effects of some heavy metals. *Interdiscip. Toxicol.* **2014**, *7*, 60–72. [CrossRef] [PubMed]
2. Sheela, T.; Nayaka, Y.A.; Viswanatha, R.; Basavanna, S.; Venkatesha, T.G. Kinetics and thermodynamics studies on the adsorption of Zn(II), Cd(II) and Hg(II) from aqueous solution using zinc oxide nanoparticles. *Powder Technol.* **2012**, *217*, 163–170. [CrossRef]
3. Mohamed, H.S.; Soliman, N.K.; Abdelrheem, D.A.; Ramadan, A.A.; Elghandour, A.H.; Ahmed, S.A. Adsorption of Cd^{2+} and Cr^{3+} ions from aqueous solutions by using residue of *Padina gymnospora* waste as promising low-cost adsorbent. *Heliyon* **2019**, *5*, e01287. [CrossRef] [PubMed]
4. Gu, M.; Hao, L.; Wang, Y.; Li, X.; Chen, Y.; Li, W.; Jiang, L. The selective heavy metal ions adsorption of zinc oxide nanoparticles from dental wastewater. *Chem. Phys.* **2020**, *534*, 110750. [CrossRef]
5. Kumar, K.Y.; Muralidhara, H.B.; Nayaka, Y.A.; Balasubramanyam, J.; Hanumanthappa, H. Low-cost synthesis of metal oxide nanoparticles and their application in adsorption of commercial dye and heavy metal ion in aqueous solution. *Powder Technol.* **2013**, *246*, 125–136. [CrossRef]
6. Azizi, S.; Mahdavi Shahri, M.; Mohamad, R. Green synthesis of zinc oxide nanoparticles for enhanced adsorption of lead ions from aqueous solutions: Equilibrium, kinetic and thermodynamic studies. *Molecules* **2017**, *22*, 831. [CrossRef] [PubMed]
7. Nalwa, K.; Thakur, A.; Sharma, N. Synthesis of ZnO nanoparticles and its application in adsorption. *Adv. Mater. Proc.* **2017**, *2*, 697–703. [CrossRef]
8. Mesquita Vieira, D.; Augusto da Costa, A.C.; Assumpção Henriques, C.; Luiz Cardoso, V.; Pessôa de França, F. Biosorption of lead by brown seaweed *Sargassum filipendula*—Batch and continuous pilot studies. *Electron. J. Biotechnol.* **2007**, *10*, 368–375. [CrossRef]
9. Benaisa, S.; Arhoun, B.; El Mail, R.; Rodriguez-Maroto, J.M. Potential of brown algae biomass as new biosorbent of iron: Kinetic, equilibrium and thermodynamic study. *J. Mater. Environ. Sci.* **2018**, *9*, 2131–2141.
10. Barquilha, C.E.R.; Cossich, E.S.; Tavares, C.R.G.; Silva, E.A. Biosorption of nickel (II) and copper (II) ions in batch and fixed-bed columns by free and immobilized marine algae *Sargassum* sp. *J. Clean. Prod.* **2017**, *150*, 58–64. [CrossRef]
11. Cossich, E.S.; Tavares, C.R.G.; Ravagnani, T.M.G. Biosorption of chromium(III) by *Sargassum* sp. biomass. *Electron. J. Biotechnol.* **2002**, *5*, 6–7. [CrossRef]
12. Cossich, E.S.; da Silva, E.A.; Tavares, C.R.G.; Ravagnani, T.M.G. Biosorption of chromium (III) by biomass of seaweed *Sargassum* sp. in a fixed-bed column. *Adsorption* **2004**, *10*, 129–138. [CrossRef]
13. Tamilselvan, N.; Saurav, K.; Kannabiran, K. Biosorption of Cr (VI), Cr (III), Pb (II) and Cd (II) from aqueous solutions by *Sargassum wightii* and *Caulerpa racemose* algal biomass. *J. Ocean Univ. China* **2012**, *11*, 52–58. [CrossRef]
14. Wang, Y.; Li, Y.; Zhao, F.J. Biosorption of chromium(VI) from aqueous solutions by *Sargassum thunbergii* Kuntze. *Biotechnol. Biotechnol. Equip.* **2014**, *28*, 259–265. [CrossRef] [PubMed]
15. Azizi, S.; Ahmad, M.B.; Namvar, F.; Mohamad, R. Green biosynthesis and characterization of zinc oxide nanoparticles using brown marine macroalga *Sargassum muticum* aqueous extract. *Mater. Lett.* **2014**, *116*, 275–277. [CrossRef]
16. Rupa, E.J.; Anandapadmanaban, G.; Mathiyalagan, R.; Yang, D.C. Synthesis of zinc oxide nanoparticles from immature fruits of *Rubus coreanus* and its catalytic activity for degradation of industrial dye. *Optik* **2018**, *172*, 1179–1186. [CrossRef]
17. Akintelu, S.A.; Folorunso, A.S. A review on green synthesis of zinc oxide nanoparticles using plant extracts and its biomedical applications. *BioNanoScience* **2020**, *10*, 848–863. [CrossRef]

18. Elrefaey, A.A.K.; El-Gamal, A.D.; Hamed, S.M.; El-belely, E.F. Algae-mediated biosynthesis of zinc oxide nanoparticles from *Cystoseira crinite* (*Fucales; Sargassaceae*) and it's antimicrobial and antioxidant activities. *Egypt. J. Chem.* **2022**, *65*, 231–240. [CrossRef]
19. Dziergowska, K.; Wełna, M.; Szymczycha-Madeja, A.; Chęcmanowski, J.; Michalak, I. Valorization of *Cladophora glomerata* biomass and obtained bioproducts into biostimulants of plant growth and as sorbent (biosorbents) of metal ions. *Molecules* **2021**, *26*, 6917. [CrossRef]
20. Bertagnolli, C.; de Silva, M.G.; Guibal, E. Chromium biosorption using the residue of alginate extraction from *Sargassum filipendula*. *Chem. Eng. J.* **2014**, *237*, 362–371. [CrossRef]
21. Cardoso, S.L.; Costa, C.S.D.; Nishikawa, E.; da Silva, M.G.C.; Vieira, M.G.A. Biosorption of toxic metals using the alginate extraction residue from the brown algae *Sargassum filipendula* as a natural ion-exchanger. *J. Clean. Prod.* **2017**, *165*, 491–499. [CrossRef]
22. Vaishnav, J.; Subha, V.; Kirubanandan, S.; Arulmozhi, M.; Renganathan, S. Green synthesis of zinc oxide nanoparticles by *Celosia argentea* and its characterization. *J. Optoelectron. Biomed. Mater.* **2017**, *9*, 59–71.
23. Brand-Williams, W.; Cuvelier, M.E.; Berset, C.L.W.T. Use of a free radical method to evaluate antioxidant activity. *LWT Food Sci. Technol.* **1995**, *28*, 25–30. [CrossRef]
24. Papirio, S.; Frunzo, L.; Mattei, M.R.; Ferraro, A.; Race, M.; D'Acunto, B.; Pirozzi, F.; Esposito, G. Heavy Metal Removal from Wastewaters by Biosorption: Mechanisms and Modeling. *Environ. Chem. A Sustain. World* **2017**, *8*, 25–63. [CrossRef]
25. Michalak, I.; Chojnacka, K. The new application of biosorption properties of *Enteromorpha prolifera*. *Appl. Biochem. Biotechnol.* **2010**, *160*, 1540–1556. [CrossRef]
26. Cazón, J.P.H.; Benítez, L.; Donati, E.; Viera, M. Biosorption of chromium(III) by two brown algae *Macrocystis pyrifera* and *Undaria pinnatifida*: Equilibrium and kinetic study. *Eng. Life Sci.* **2012**, *12*, 95–103. [CrossRef]
27. Martín, A.P.; Aguilar, M.I.; Meseguer, V.F.; Ortuno, J.F.; Sáez, J.; Lloréns, M. Biosorption of chromium (III) by orange (*Citrus cinensis*) waste: Batch and continuous studies. *Chem. Eng. J.* **2009**, *155*, 199–206. [CrossRef]
28. Jha, D.; Haider, M.B.; Kumar, R.; Byamba-Ochir, N.; Shim, W.G.; Marriyappan Sivagnanam, B.; Moon, H. Enhanced adsorptive desulfurization using Mongolian anthracite-based activated carbon. *ACS Omega* **2019**, *4*, 20844–20853. [CrossRef] [PubMed]
29. Dada, A.O.; Olalekan, A.P.; Olatunya, A.M.; Dada, O.J. Langmuir, Freundlich, Temkin and Dubinin–Radushkevich isotherms studies of equilibrium sorption of Zn^{2+} unto phosphoric acid modified rice husk. *IOSR J. Appl. Chem.* **2012**, *3*, 38–45. [CrossRef]
30. Jin, X.; Liu, Y.; Tan, J.; Owens, G.; Chen, Z. Removal of Cr(VI) from aqueous solutions via reduction and absorption by green synthesized iron nanoparticles. *J. Clean. Prod.* **2018**, *176*, 929–936. [CrossRef]
31. Bourebaba, L.; Michalak, I.; Röcken, M.; Marycz, K. *Cladophora glomerata* methanolic extract decreases oxidative stress and improves viability and mitochondrial potential in equine adipose derived mesenchymal stem cells (ASCs). *Biomed. Pharmacother.* **2019**, *111*, 6–18. [CrossRef] [PubMed]
32. Fazlzadeh, M.; Khosravi, R.; Zarei, A. Green synthesis of zinc oxide nanoparticles using *Peganum harmala* seed extract, and loaded on *Peganum harmana* seed powdered activated carbon as new adsorbent for removal of Cr(VI) from aqueous solution. *Ecol. Eng.* **2017**, *103*, 180–190. [CrossRef]
33. Guarín-Romero, J.R.; Rodríguez-Estupiñán, P.; Giraldo, L.; Moreno-Piraján, J.C. Simple and competitive adsorption study of nickel (II) and chromium (III) on the surface of the brown algae *Durvillaea antarctica* biomass. *ACS Omega* **2019**, *4*, 18147–18158. [CrossRef] [PubMed]
34. Ortiz-Calderon, C.; Silva, H.C.; Vasquez, D.B. Metal removal by seaweed biomass. In *Biomass Volume Estimation and Valorization for Energy*; INTECH: London, UK, 2017; pp. 362–389. [CrossRef]